

A Novel Machine-Learning Framework-based on LBP and GLCM Approaches for CBIR System

Meenakshi Garg¹, Manisha Malhotra¹, and Harpal Singh²

¹University Institute of Computing, Chandigarh University, India

²Department of Electronics and Communication Engineering, CEC Landran, India

Abstract: This paper presents a Multiple-features extraction and reduction-based approaches for Content-Based Image Retrieval (CBIR). Discrete Wavelet Transforms (DWT) on colored channels is used to decompose the image at multiple stages. The Gray Level Co-occurrence Matrix (GLCM) concept is used to extract statistical characteristics for texture image classification. The definition of shared knowledge is used to classify the most common features for all COREL dataset groups. These are also fed into a feature selector based on the particle swarm optimization which reduces the number of features that can be used during the classification stage. Three classifiers, called the Support Vector Machine (SVM), K-Nearest Neighbor (KNN) and Decision Tree (DT), are trained and tested, in which SVM give high classification accuracy and precise rates. In several of the COREL dataset types, experimental findings have demonstrated above 94 percent precision and 0.80 to 0.90 precision values.

Keywords: CBIR, DWT, SHO, feature selection, classification.

Received November 18, 2019; accepted July 20, 2020

<https://doi.org/10.34028/iajit/18/3/5>

1. Introduction

Content-Based Image Retrieval (CBIR) is the most important field of computer vision and image processing. It is used in different fields, such as medicine, health, cultural heritage, prevention of crime, etc. Based on its visual content, the CBIR is a well-defined searching and recovery technique in a broad dataset. The recovery of images is characterized by local or global visual content characteristics. The characteristics of the images, such as color, shape and texture, describe global characteristics [41]. Color is a common visual function used in CBIR and is primarily studied in literature (see Figure 1). The main goal is for people, particularly in color lines, to distinguish pictures [47]. Texture is also an important aspect of image surfaces and is characterized by visual patterns similarity, reflecting the most significant details on the image surface as bricks, carvings, clouds etc., These descriptors are also suitable for medical pictures recovery. The type descriptors do not imply that the entire picture is described, but rather, that the structure of the specific part of an image is described. In order to identify and classify object categories and collect points of concern and areas, local image characteristics were used effectively. Since, the 1990s images recovery from datasets have become a particularly dynamic research topic with visual content. Nonetheless, the semanticized dimension of images, which comprises the fundamental semantic difference between device results and user experience, is still not sufficiently considered in most trials. First, of all, an

image element is extracted and features are picked. The second is the estimation of the similarity measures [42]. Eventually, function indexing and recovery is carried out. The way the characteristics are extracted and picked depends on the area of the image or the whole image. Descriptors are often evaluated by using the spatial information texture, shape and colors etc., The use of local descriptors has increased in recent years since they continue to be used in similar ways, as the local descriptors are extracted from the areas of the image, rather than from the whole image. In addition, local descriptors are extracted from the image in which the Scale Invariant Feature Transform (SIFT) [34], Speeded Up Robust Features (SURF) [4], Histogram of Oriented Gradient (HoD) [9] and Local-Binary patterns [39] are used specifically for CBIR. In addition to these LBP versions, the traditional Local Binary Patterns [44] were proposed as an efficient version of these DFLs. The calculation of similitude is the second and major phase of the CBIR models. It attempts to reduce the semantic difference [19]. In the first few years of the CBIR, the focus was put on the various similarity measures required for each particular function. For calculation of the resemblance between image descriptors, similarity measures such as Mahalanobis and Euclidean distances are used. Instead of calculating the recent use of similarities [34], learning of similarities has become popular [10]. However, in modern research for CBIR machine learning is becoming popular [35].

By taking large datasets for training [12, 40], the system efficiency could be improved. Synthetic

Aperture Radar (SAR) is typically used in second stage CBIR approaches over the last few years. The input signals with a simple combination are a dictionary-based collection of dispersed coefficients [5, 6].

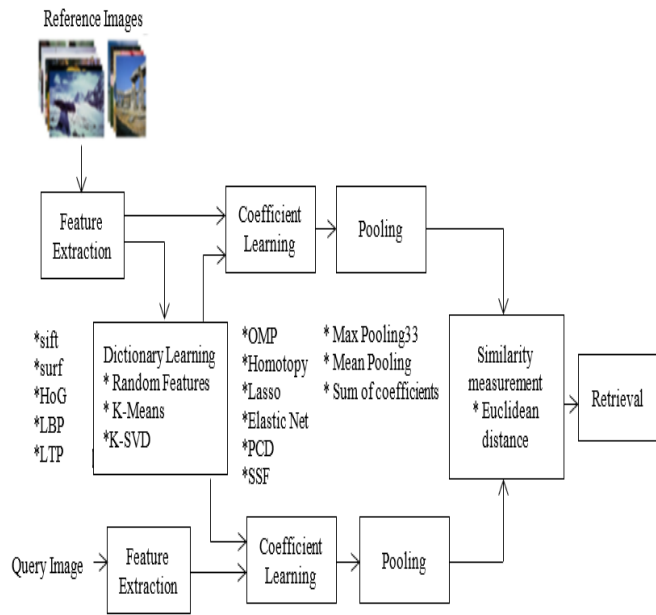


Figure 1. CBIR framework.

In this paper, we designed and developed a novel CBIR based approach for image retrieval on the basis of classification. The proposed method is compared and analyzed with various well-known machine-learning models. The results show the superiority of the proposed method [2, 3].

The rest of this paper is structured as follow: section 2 presents the related work. The feature extraction is discussed in section 3. In section 4, feature selection using Particle Swarm Optimization (PSO) algorithm is presented. The results and discussions are discussed in section 5 followed by the conclusions and future work in section 6.

2. Related Works

Local Binary Pattern (LBP) texture features are based on local features since the pixel value of borders is different in the window to the oriented reference pixel and are weighted in the various directions. The textures are based on the local features. In the meantime, incorrect models for irregular shapes and textures have been created with the local binary pattern. A treatment of dominant low back pain is suggested in [14]. The local binary Dominant style is better than the local binary pattern for image rotation and histograms equalization. Ahonen and Pietikinen [1] proposed that a local binary pattern variance descriptor be used to retain global spatial image information. They then built up a more comprehensive descriptor of local binary patterns for local texture features than typical local binary patterns [31]. On the basis of the local binary pattern combination and the hair wavelets, a variety of

Haar Local Binary Model features (LBHP) have been suggested [32]. In Haar LBHP, instead of measuring a variance of amplitude between the neighboring and the related pixels, the polarity of variance is considered. The histograms flexibly resistant to noise in LBP and Sign Local Binary Pattern (SLBP) compared with traditional LBP as suggested in [7]. Chandrasekhar *et al.* [8] suggested a Fuzzy Local Binary Pattern (FLBP) configuration, a new type of LBP, which reflects the fuzzy logic of the local texture patterns. The Oriented Gradient Histogram (HOG) extracts local information texture characteristics which depend on local intensity gradient distribution and fits in object detection applications [46]. Tan and Triggs [44] proposed a low-throughput HOG-type compressed method. Several HOG compressed schemes are subsequently shown [48]. Guo *et al.* [25] have shown that a variety of databases have substantially enhanced recovery efficiency by integrating LBP and HOG characteristics [15] have shown that LBP characteristics in uniform, Local Ternary-based models have been highly noise-sensitive and have been implemented [16, 17] showed a local derivative model in which profound data are derived with or above second-order derivatives [43] used a Local-Directional drift model in which the histogram pattern is built as characteristics to achieve invariant rotational characteristics. Nonetheless, without regard to the Local Line Directional Pattern (LDDP) address [38], the derivative order of the reference pixel and its neighbor pixel is determined. The characteristics obtained from these methods are based simply on the positive and negative edge directions. Moreover, the edges in multiple directions can be differentiated to obtain a higher output. Liu *et al.* [36] has shown that the accuracy of the medical image retrieval can be enhanced by using Fourier transformation into local ternary patterns due to its high redundancy. In the local standard vector [37] used, by combining these derivatives, to generate Local Vector Pattern (LVP) models by calculating multiple point derivatives in each of the directions. A new algorithm is implemented to the size of function vectors in comparative space transformations [18, 20]. The Comparative Space Transformation extracts the functions with more details and also with noise tolerance through the implementation of a linear-dynamic decision system [11].

The Comparative Space Transformation extracts these functions with more details and also immune to noise through the implementation of a linear dynamic decision function. Generally, Local binary pattern (LBP), Linguistic Indexing of Pictures (LIP), Local Derivative Pattern (LDP), Local Tetra Patterns (LTrP), Local Vector Pattern (LVP) are the variations, rest on the referenced pixel and nearest to the gray pixel and neighbor degree. These patterns are classified as various things in the cycle or square as different combinations of gray pixels. Text can be seen in a

variety of intensities in the direction of natural system elements with a limited ability to display texture data. Added pixel elements and beyond 3 or 4 computations and harmful to the details of the image to the last encoding. The more image data is thus obtained when encoding at multiple levels is used rather than binary code.

3. Feature Extraction

The feature extraction and classification are given in Figures 3 and 4.

3.1. DWT

Wavelets are the low frequency waves. It is very small in length [45]. These are used in multi-resolution analysis. All images are processed and viewed at different resolution. At high resolution, tiny and low-contrast objects are observed and large, high-contrast objects on the ground level are analyzed [26].

A contracted, high-frequency basis function is used for temporal analysis, and a dilated, low-frequency basis function is used for frequency analysis in wavelet analysis. One of the Daubechies wavelets is the Haar wavelet (Daubechies-1). Because of its simple interpolation schema, it is very commonly used technique. If you're looking for a unique Wavelet uses two different types of filters are used. The first is a low-pass filter, and the second is a high-pass filter. One can easily conclude that the low-pass filter contains more information than since the majority of the signal energy is concentrated in low-pass filter, high-pass filter is used. Daubechies-4 wavelet, on the other hand, splits the input signal by using four kinds of filter (LL, LH, HL, HH) with most of the energy concentrating in LL sub-band Where (L stands for low, while H stands for high).

3.2. Dominant Rotated Local Binary Pattern (DRLBP)

This is an effective invariant texture rotation descriptor that is used with median local binary patterns in the functional extraction phase. This property is achieved by measurement of the descriptor with a reference to a local pixel high. This path of Dominant is invariant with the monotonous gray value [27].

3.3. Median Robust Extended Local Binary Pattern (MRELBP)

Dhiman *et al.* [13], proposed the Extended Local Binary Pattern (ELBP) process, using a center-pixel intensity, neighborhood-pixel intensity, radial differences and angular differences as four descriptors close to LBP. The key difference between the method of ELBP and the method of Median Robust Extended Local Binary pattern (MRELBP) [28]. Only the values

of a single pixel are used in the ELBP procedure, while a window, scaled and medium approach is used in the MRELBP procedure.

1. MRELBP CI

$$MRELBP_CI(x_c) = s(\phi X_{c,w}) - \mu_w \quad (1)$$

Where $X_{c,w}$ represents local-patch centered around central pixel X_c considered for feature extraction and the function $\phi(X)$ determine median of local-patch and μ_w is the mean of the image.

2. MRELBP NI

$$MRELBP_NI_{ra,p}(x_c) = \sum_{n=0}^{p-1} S(\phi(X_{ra,p,w_{ra},n}) - \mu_{ra,p,w_{ra}})2^n$$

$$\mu_{ra,p,w_{ra}} = \frac{1}{p} \sum_{n=0}^{p-1} \phi(X_{ra,p,w_{ra},n}) \quad (2)$$

Where $X_{ra,p,w_{ra},n}$ denotes the patch of size $w_{ra} \times w_{ra}$ centered at pixel $X_{ra,p,n}$

3. MRELBP RD

$$MRELBP_RD_{ra,ra-1,p,w_r,w_r-1} = \sum_{n=0}^{p-1} S(\phi(X_{ra,p,w_r,n}) - \phi(X_{ra-1,p,w_{ra-1},n}))2^n \quad (3)$$

Where $X_{ra,p,w_{ra},n}$ denotes the patches around neighbor pixels $x_{ra,p,n}$ arranged on circle around centered pixel x_c having radius ra , and S represents the segments [29].

3.4. Gray Level Co-Occurrence Matrix

This transforms the host image into the matrix that responds with a certain distance to the reference of the pixel values [30]. This assessed the mutual occurrence of two-pixel pair values with different distances and directions which consider horizontal, vertical, and diagonal directions.

$$G_{dist}^{theta}(i, j) = \{(x, y), (m, n) | I(x, y) = i, I(m, n) = j\} \quad (4)$$

where $(x, y), (m, n) \in N_x \times N_y$

$$(m, n) = (x + dist \times theta_1, y + dist \times theta_2) \quad (5)$$

Where G_{dist}^{theta} is the gray-level co-occurrence matrix of distance $dist$ and angle $theta$. $I(x, y)$ and $I(m, n)$ are the pixel intensity at position (m, n) . Values of $theta_1$ and $theta_2$ are depend upon direction.

In current plays, local binary patterns are typically called histograms for extraction, and their frequency does not involve the pattern. By using Gray Level Co-occurrence Matrix (GLCM) in various directions and lengths, the Dominant Rotated Local Binary Pattern (DRLBP) feature extraction process is implemented [33].

$$Img = DRLBP(dwtcoefficients)$$

$$GLCM_{dist}^{theta}(Img) = G_{dist}^{theta}(i, j) \forall (i, j) \in Img \quad (6)$$

Where Img is the *DRLBP* image-map. Four combinations of *GLCM* as explained above, have been used to create four different feature vectors.

$$FV_1(I) [GLCM_1^{0^\circ} GLCM_1^{45^\circ} GLCM_1^{90^\circ} GLCM_1^{135^\circ}] \quad (7)$$

$$FV_2(I)[GLCM_2^{0^\circ} GLCM_2^{45^\circ} GLCM_2^{90^\circ} GLCM_2^{135^\circ}] \quad (8)$$

$$FV_3(I)[GLCM_1^{0^\circ} GLCM_1^{45^\circ} GLCM_2^{90^\circ} GLCM_2^{45^\circ}] \quad (9)$$

$$FV_4(I)[GLCM_1^{0^\circ} GLCM_1^{90^\circ} GLCM_2^{0^\circ} GLCM_2^{90^\circ}] \quad (10)$$

More spatial information is available in neighboring pixels that extract frequency of these patterns in other directions by obtaining GLCM in specific directions and distances [21, 22, 24].

4. Feature Selection Using Spotted Hyena Optimizer (ShO)

This section describes the feature selection by using the Spotted Hyena Optimizer (SHO) in detail.

4.1. Proposed Spotted Hyena Optimizer

$$\vec{D}_h = |\vec{B} \cdot \vec{P}_p(x) - \vec{P}(x)| \quad (11)$$

$$\vec{P}(x+1) = \vec{P}_p(x) - \vec{E} \cdot \vec{D}_h \quad (12)$$

Where D_h defines the distance between the prey and spotted hyena, x indicates the current iteration, B and E are co-efficient vectors, P_p indicates the position vector of prey, P is the position vector of spotted hyena. The vectors B and E are calculated as follows [35]:

$$\vec{B} = 2 \cdot r \cdot \vec{d}_1 \quad (13)$$

$$\vec{E} = 2 \cdot \vec{h} \cdot r \cdot \vec{d}_2 - \vec{h} \quad (14)$$

$$\vec{h} = 5 - (\text{Iteration} \times (5 / \text{Max}_{\text{Iteration}})) \quad (15)$$

Where, $\text{Iteration} = 1, 2, 3, \dots, \text{Max}_{\text{Iteration}}$

$$\vec{D}_h = |\vec{B} \cdot \vec{P}_h - \vec{P}_k| \quad (16)$$

$$\vec{P}_k = \vec{P}_h - \vec{E} \cdot \vec{D}_h \quad (17)$$

$$\vec{C}_h = \vec{P}_k + \vec{P}_{k+1} + \dots + \vec{P}_{k+N} \quad (18)$$

Where P_h defines the position of first best spotted hyena, P_k indicates the position of other spotted hyenas. Here, N indicates the number of spotted hyenas which is computed as follows:

$$N = \text{count}_{\text{nos}}(\vec{P}_h, \vec{P}_{h+1}, \vec{P}_{h+2}, \dots, (\vec{P}_h + \vec{M})) \quad (19)$$

Where M is a random vector lies in the range of [0.5, 1], nos defines the number of solutions and count all candidate solutions, after addition with M , which are far similar to the best optimal solution in a given search space, and C_h is a group or cluster of N number of optimal solutions.

$$\vec{P}(x+1) = \frac{\vec{C}_h}{N} \quad (20)$$

Where $P(x+1)$ save the best solution and updates the positions of other search agents according to the position of the best search agent [23]. The SHO

algorithm allows its search agents to update their position and attack towards the prey (see Figure 2).

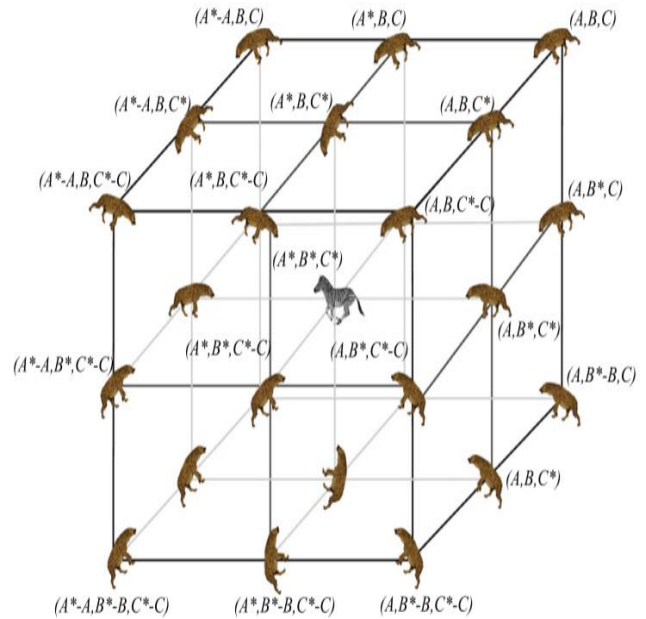


Figure 2. Spotted hyena optimizer.

5. Proposed Model

The proposed model of this work is described in the Figures 3, 4, and 5. In Figure 3 of the working model of hybrid support vector based feature extraction descriptor. Firstly, Red Green Blue (RGB) image is divided into red, green and blue channels. Then Discrete Wavelet Transforms (DWT) is applied to these channels. In Figure 4 of the proposed method, you can see that the training dataset i.e., 70% is taken from phase-II and testing dataset is considered as 30%.

Then three classifiers are used that is SVM, K-Nearest Neighbor (KNN), and Decision Tree (DT). All these classifiers are considered one by one for the extraction of efficient classified images.

The overall functioning and flowchart of the proposed method is given in the Figure 5. At the end, finally the optimal features are extracted and concatenated.

PHASE-I

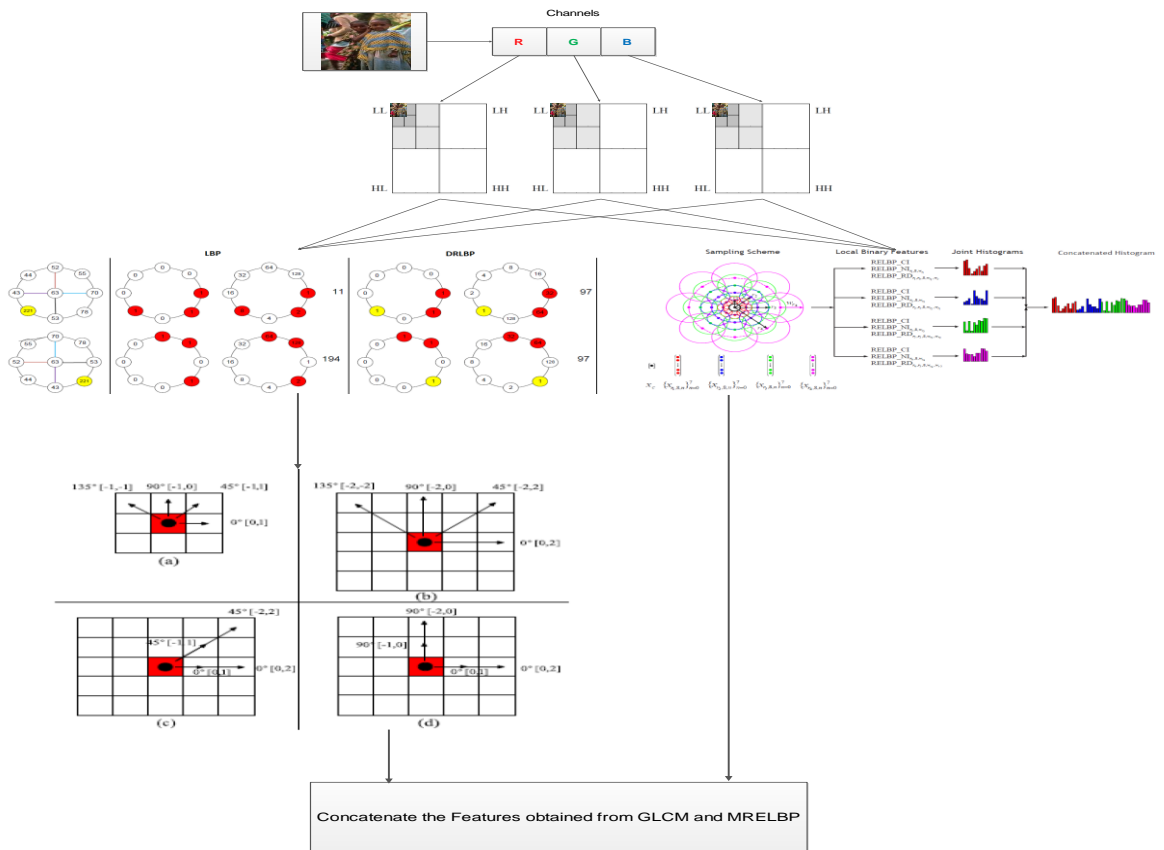


Figure 3. Working of proposed feature extraction model.

PHASE-III

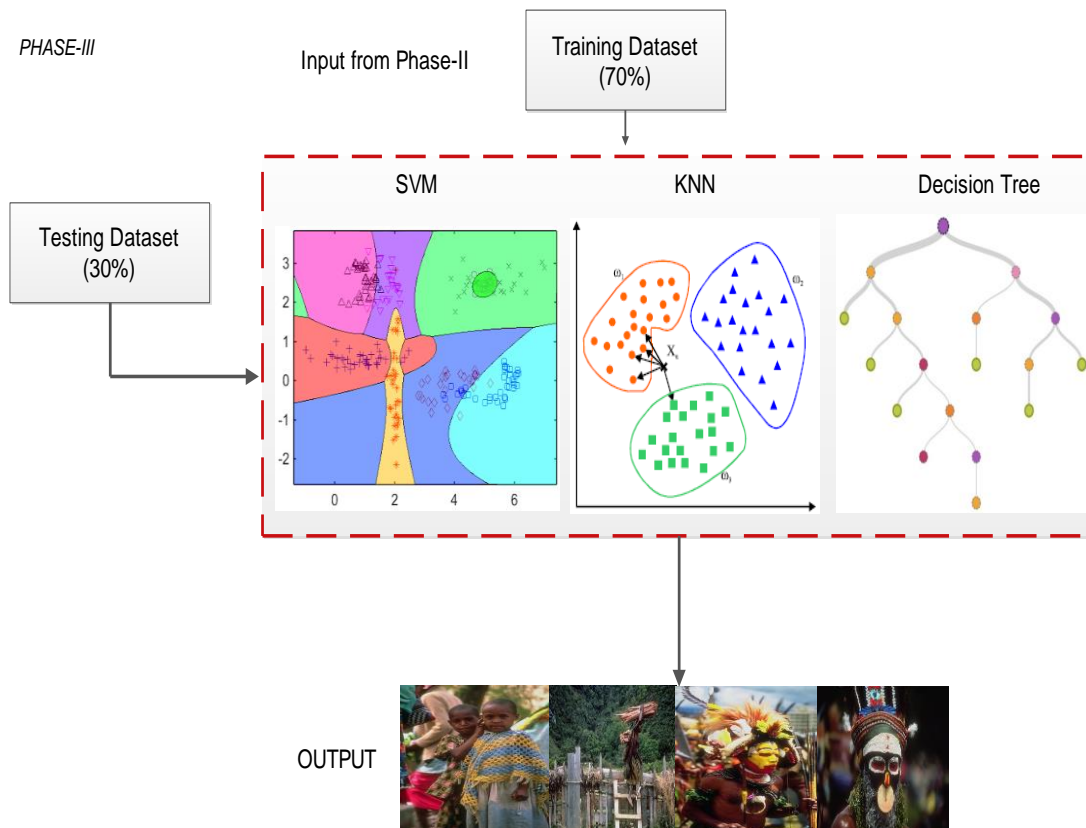


Figure 4. Working of proposed classification model.

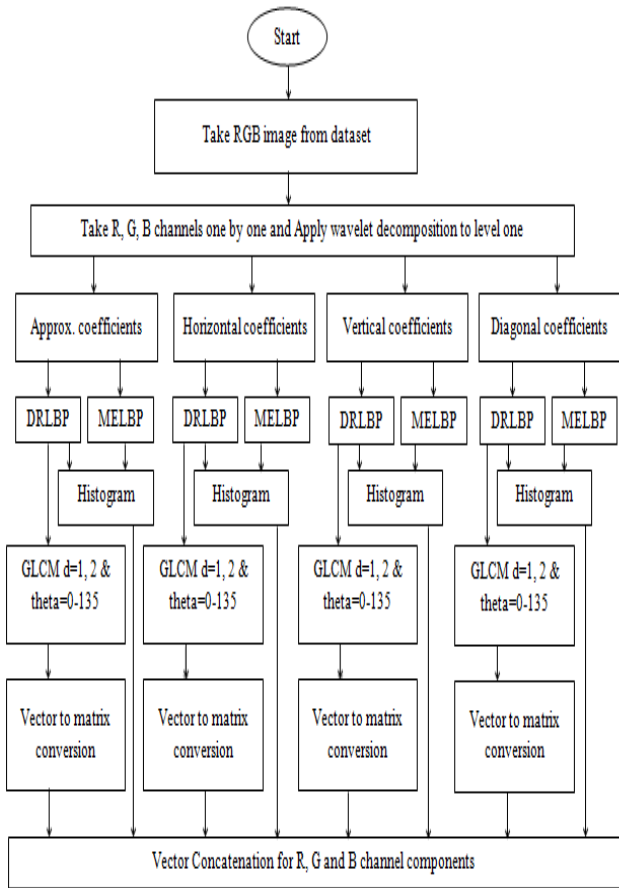


Figure 5. Flowchart of proposed model.

6. Results and Discussion

A general WANG dataset was used to test the proposed process, which includes 1000 core images with 10 distinct subject categories. It can be obtained in Joint Photographic Experts Group (JPEG) format from size 384 x 256 or 256 x 384.

Along with recall, precision, F-measure and Accuracy parameters are also used. The formulas

$$Precision = \frac{True_Positive}{(True_Positive + False_positive)} \quad (21)$$

$$Recall = \frac{True_positive}{(True_positive + False_negative)} \quad (22)$$

$$F_Measurement = \frac{2 * Precision * Recall}{(Precision + Recall)} \quad (23)$$

$$Accuracy = \frac{True_Positive + True_Negative}{(True_Positive + True_Negative + False_positive + True_Negative)} \quad (24)$$

According to results mentioned in Table 1 and Figure 6, SVM obtains high recall ratio for all 10 in which Beaches, Building, Food and mountain category have 0.86, 0.89, .86 and .92 recall values. Decision tree and kNN classifiers have significantly low values of recall parameter as compared to SVM classifier. From Table 2 and Figure 7, it can be seen that SVM gives efficient precision value for almost all categories in which beaches, flowers, horses and mountain has high

measured values of precision noted as 0.94, .85, .85, and 0.89, respectively.

Table 1. Performance evaluation of CBIR using Decision Tree classifier.

Parameters	TP	TN	FP	FN	Precision	Recall	F-Measure	Accuracy
Class	Classification Results Using Decision Tree							
Africa	65	867	33	32	0.661	0.64	0.643	0.991
Beaches	74	841	59	25	0.559	0.73	0.644	0.915
Building	64	862	32	36	0.631	0.64	0.636	0.927
Bus	66	884	16	34	0.804	0.62	0.724	0.925
Dinosaur	63	871	22	30	0.744	0.64	0.688	0.945
Elephant	70	867	32	30	0.671	0.71	0.684	0.935
Flowers	75	851	48	24	0.612	0.760	0.678	0.925
Food	66	887	13	30	0.831	0.661	0.734	0.953
Horses	66	851	43	33	0.582	0.670	0.623	0.915
Mountain	59	882	14	40	0.761	0.591	0.664	0.941

Table 2. Performance evaluation of CBIR using k-Nearest Neighbor.

Parameters	TP	TN	FP	FN	Precision	Recall	F-Measure	Accuracy
Class	Classification Results Using K-Nearest Neighbor							
Africa	76	781	119	22	0.394	0.79	0.530	0.862
Beaches	58	827	72	42	0.446	0.53	0.502	0.873
Building	66	832	72	32	0.469	0.62	0.534	0.892
Bus	59	860	42	41	0.596	0.55	0.592	0.919
Dinosaur	56	842	58	46	0.482	0.54	0.509	0.894
Elephant	47	862	36	52	0.564	0.46	0.512	0.911
Flowers	46	879	22	58	0.666	0.43	0.515	0.922
Food	68	882	18	32	0.796	0.68	0.732	0.911
Horses	26	897	06	72	0.828	0.25	0.429	0.923
Mountain	51	888	12	42	0.806	0.52	0.622	0.932

Table 3. Performance evaluation of CBIR using support vector machine.

Parameters	TP	TN	FP	FN	Precision	Recall	F-Measure	Accuracy
Class	Classification Results Using SVM							
Africa	83	883	16	18	0.815	0.83	0.813	0.964
Beaches	87	896	04	15	0.956	0.87	0.910	0.983
Building	93	873	25	10	0.785	0.90	0.833	0.964
Bus	80	884	14	25	0.833	0.83	0.816	0.964
Dinosaur	73	883	17	21	0.822	0.79	0.803	0.962
Elephant	83	876	24	17	0.775	0.83	0.801	0.959
Flowers	82	887	12	15	0.865	0.83	0.843	0.969
Food	83	883	14	13	0.861	0.87	0.865	0.973
Horses	82	887	14	15	0.865	0.83	0.843	0.963
Mountain	93	893	10	07	0.902	0.93	0.916	0.983

SVM classifier has high value of F-score for all tested categories. Bus, dinosaur, and elephants categories have F-score value close to 0.80 whereas beaches and mountain classes shows 0.916 F-score value. Table 3 and Figure 8 show the results for support vector machine.

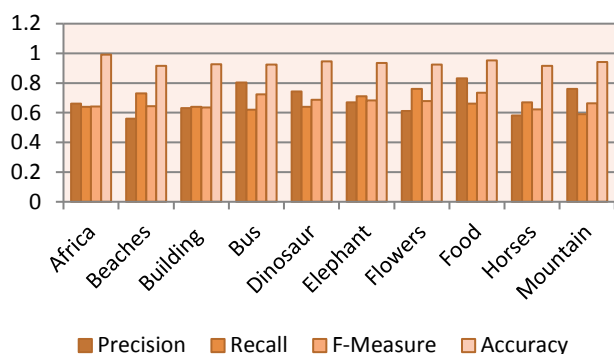


Figure 6. Bar graphs for decision tree classifier on Corel Dataset.

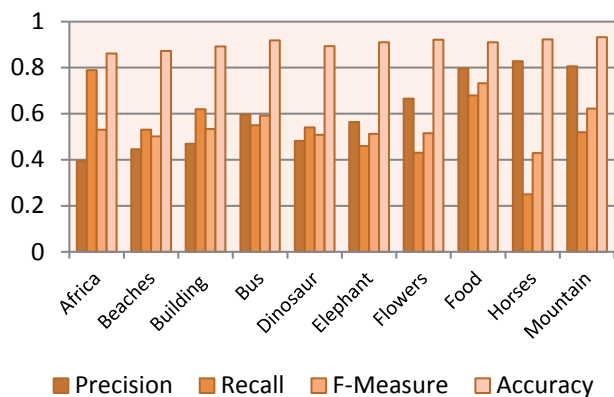


Figure 7. Bar graphs for k-nearest neighbor on Corel Dataset.

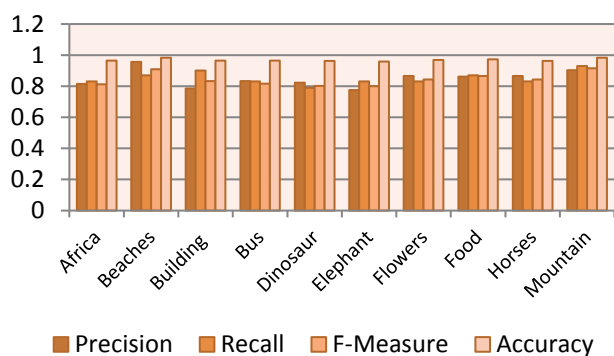


Figure 8. Bar graphs for support vector machine on Corel Dataset.

7. Conclusions

In this experiment, multiple extractions were performed using SHO optimizer, which extracts the most differentiating functions. The Corel dataset consists of ten categories and displays the classification results by means of four presentation parameters, i.e., precision, precision, f-score and recall, of which three classification methods are used to assist the vector machine, decision tree and k-classification neighbor. For determining its objective purpose, SHO uses SVM classifier to optimize the Area Under Curve (AUC) average for the features selected. SHO aims to raise the AUC value for all groups and gives a strong AUC value to the function vector when defined by SVM. Experimental results show SVM to be the best that shows high recall values, F-score and precision parameters. One of the

disadvantages of proposed approach is its time complexity. So, this limitation can be seen as future contribution for the researchers. Moreover, researchers are trying to develop this model in their upcoming research [32-46].

Conflict of Interest

The authors declare that they have no conflict of interest.

References

- [1] Ahonen T. Pietikinen M., "Soft Histograms for Local Binary Patterns," *Proceedings of the Finnish Signal Processing Symposium*, vol. 5, no. 9, pp. 1-4, 2007.
- [2] Amin A. and Qureshi M., "A Novel Image Retrieval Technique Using Automatic and Interactive Segmentation," *The International Arab Journal of Information Technology*, vol. 17, no. 3, pp. 404-410, 2020.
- [3] Bul S., Rabbi M., and Pelillo M., "Content-Based Image Retrieval with Relevance Feedback Using Random Walks," *Pattern Recognition*, vol. 44, no. 9, pp. 2109-2122, 2011.
- [4] Bay H., Ess A., Tuytelaars T., and Gool L., "Speeded-up Robust Features (SURF)," *Computer Vision Image Understanding*, vol. 110, no. 3, pp. 346-359, 2008.
- [5] Bhukya R. and Ashok A., "Gene Expression Prediction Using Deep Neural Networks," *The International Arab Journal of Information Technology*, vol. 17, no. 3, pp. 422-431, 2020.
- [6] Chang H. and Yeung D., "Locally Linear Metric Adaptation with Application to Semi-Supervised Clustering and Image Retrieval," *Pattern Recognition*, vol. 39, no. 7, pp.1253-1264, 2006.
- [7] Chandrasekhar V., Takacs G., Chen D., Tsai S., Grzeszczuk R., and Girod B., "CHog: Compressed Histogram of Gradients A Low Bit-Rate Feature Descriptor," in *Proceedings of the IEEE Conference on Computer Vision and Pattern Recognition*, Miami, pp. 2504-2511, 2009.
- [8] Chandrasekhar V., Reznik Y., Takacs G., Chen D., Tsai S., Grzeszczuk R., and Girod B., "Quantization Schemes for Low Bitrate Compressed Histogram of Gradients Descriptors," in *Proceedings of the IEEE Computer Society Conference on Computer Vision and Pattern Recognition-Workshops*, San Francisco, pp. 33-40, 2010.
- [9] Dalal N. and Triggs B., "Histograms of Oriented Gradients for Human Detection," in *Proceedings of the IEEE Computer Society Conference on Computer Vision and Pattern Recognition*, San Diego, pp. 886-893, 2005.

- [10] Dalal N., and Tariggs B., and Schmid C., "Human Detection Using Oriented Histograms of Flow and Appearance," in *Proceedings of European Conference on Computer Vision*, Graz, pp. 428-441, 2006.
- [11] Dhiman G. and Vijay K., "Spotted Hyena Optimizer: A Novel Bio-Inspired Based Metaheuristic Technique for Engineering Applications," *Advances in Engineering Software*, vol. 114, pp. 48-70, 2017.
- [12] Dhiman G., Garg M., Nagar A., Kumar V., and Dehghani M., "A Novel Algorithm for Global Optimization: Rat Swarm Optimizer," *Journal of Ambient Intelligence and Humanized Computing*, pp. 1-26, 2020.
- [13] Dhiman G., Singh K., Slowik A., Chang V., Yildiz A., Kaur A., and Garg M., "EMoSQA: A New Evolutionary Multi-Objective Seagull Optimization Algorithm for Global Optimization," *International Journal of Machine Learning and Cybernetics*, vol. 12, no. 7, pp. 571-596, 2020.
- [14] Dhiman G. and Kumar V., "Emperor Penguin Optimizer: A Bio-Inspired Algorithm for Engineering Problems," *Knowledge-Based Systems*, vol. 159, pp. 20-50, 2018.
- [15] Dhiman G. and Kumar V., "Multi-Objective Spotted Hyena Optimizer: A Multi-Objective Optimization Algorithm for Engineering Problems," *Knowledge-Based Systems*, vol. 150, pp. 175-197, 2018.
- [16] Dhiman G. and Kumar V., "Seagull Optimization Algorithm: Theory and its Applications for Large-Scale Industrial Engineering Problems," *Knowledge-Based Systems*, vol. 165, pp. 169-196, 2019.
- [17] Dhiman G. and Kaur A., "Stoa: A Bio-Inspired Based Optimization Algorithm for Industrial Engineering Problems," *Engineering Applications of Artificial Intelligence*, vol. 82, pp. 148-174, 2019.
- [18] Dhiman G., "ESA: a Hybrid Bio-Inspired Metaheuristic Optimization Approach for Engineering Problems," *Engineering with Computers*, pp. 1-31, 2019.
- [19] Dhiman G., "MOSHEPO: A Hybrid Multi-Objective Approach to Solve Economic Load Dispatch and Micro Grid Problems," *Applied Intelligence*, vol. 50, no. 1, pp. 119-137, 2020.
- [20] Dhiman G., "Multi-Objective Metaheuristic Approaches for Data Clustering in Engineering Application," PhD Theses, Deemed University, 2019.
- [21] Dhiman G., Soni M., Pandey H., Slowik A., and Kaur H., "A Novel Hybrid Hyper volume Indicator and Reference Vector Adaptation Strategies Based Evolutionary Algorithm for Many-Objective Optimization," *Engineering with Computers*, pp. 1-19, 2020.
- [22] Fan K. and Hung T., "A Novel Local Pattern Descriptor-Local Vector Pattern in High-Order Derivative Space for Face Recognition," *IEEE Transactions on Image Processing*, vol. 23, no. 7, pp. 2877-2891, 2014.
- [23] Guo Z., Zhang L., and Zhang D., "Rotation Invariant Texture Classification Using LBP Variance (LBPV) with Global Matching," *Pattern Recognition*, vol. 43, no. 3, pp. 706-719, 2010.
- [24] Guo Z., Zhang L., and Zhang D., "A Completed Modeling of Local Binary Pattern Operator for Texture Classification," *IEEE Transaction Image Processing*, vol. 19, no. 6, pp. 1657-1663, 2010.
- [25] Guo Z., Li Q., You J., Zhang D., and Liu W., "Local Directional Derivative Pattern for Rotation Invariant Texture Classification," *Neural Computer Application*, vol. 21, no. 8, pp. 1893-1904, 2012.
- [26] Garg M. and Dhiman G., "Deep Convolution Neural Network Approach for Defect Inspection of Textured Surfaces," *Journal of the Institute of Electronics and Computer*, vol. 2, no. 1, pp. 28-38, 2020.
- [27] Garg M. and Dhiman G., "A Novel Content Based Image Retrieval Approach for Classification Using Gcm Features and Texture Fused Lbp Variants," *Neural Computing and Applications*, pp. 1311-1328, 2020.
- [28] Garg M., Malhotra M., and Singh H., "Comparison of Deep Learning Techniques on Content Based Image Retrieval," *Modern Physics Letters A*, pp. 1950285, 2019.
- [29] Garg M., Singh H., and Malhotra M., "Fuzzy-NN Approach with Statistical Features for Description and Classification of Efficient Image Retrieval," *Modern Physics Letters A*, vol. 34, no. 03, pp. 1950022, 2019.
- [30] Garg M., Malhotra M., and Singh H., "Statistical Feature Based Image Classification and Retrieval Using Trained Neural Classifiers," *International Journal of Applied Engineering Research*, vol. 13, no. 8, pp. 5766-5771, 2018.
- [31] Iakovidis D., Keramidis E., and Maroulis D., "Fuzzy Local Binary Patterns for Ultrasound Texture Characterization," in *Proceedings of International Conference Image Analysis and Recognition*, Póvoa de Varzim, pp. 750-759, 2008.
- [32] Kundu M., Chowdhury M., and Bulş S., "A graph-Based Relevance Feedback Mechanism in Content-Based Image Retrieval," *Knowledge Based System*, vol. 73, pp. 254-264, 2015.
- [33] Kaur S., Awasthi L., Sangal A., and Dhiman G., "Tunicate Swarm Algorithm: A New Bio-Inspired Based Metaheuristic Paradigm for Global Optimization," *Engineering Applications*

- of *Artificial Intelligence*, vol. 90, pp. 103541, 2020.
- [34] Lowe D., "Distinctive Image Features from Scale-Invariant Key Points," *International Journal of Computer Vision*, vol. 60, no. 2, pp. 91-110, 2004.
- [35] Liao S., Law M., and Chung A., "Dominant Local Binary Patterns for Texture Classification," *IEEE Transactions Image Processing*, vol. 18, no. 5, pp. 1107-1118, 2009.
- [36] Liu L., Zhao L., Long Y., Kuang G., and Fieguth P., "Extended Local Binary Patterns for Texture Classification," *Image and Vision Computing*, vol. 30, no. 2, pp. 86-99, 2012.
- [37] Liu L., Lao S., Fieguth P., Guo Y., Wang X., and Pietikäinen M., "Median Robust Extended Local Binary Pattern for Texture Classification," *IEEE Transactions on Image Processing*, vol. 25, no. 3, pp. 1368-1381, 2016.
- [38] Mehta R. and Egiazarian K., "Dominant Rotated Local Binary Patterns (DRLBP) for Texture Classification," *Pattern Recognition Letters*, vol. 71, no. 3, pp. 16-22, 2016.
- [39] Ojala T., Pietikainen M., and Harwood D., "Performance Evaluation of Texture Measures with Classification Based on Kullback Discrimination of Distributions," in *Proceedings of 12th International Conference on Pattern Recognition*, Jerusalem, pp. 582-585, 1994.
- [40] Oberoi A., Bakshi V., Sharma R., and Singh M., "A Framework for Medical Image Retrieval Using Local Tetra Patterns," *International Journal Engineering Technology*, vol. 5, no. 1, pp. 27-36, 2013.
- [41] Schettini R., Ciocca G., and Gagliardi I., "Feature Extraction for Content-Based Image Retrieval," *Encyclopedia of Database Systems*, pp. 1115-1119, 2009.
- [42] Su S., Chen S., Li S., Li S., and Duh D., "Structured Local Binary Haar Pattern for Pixel-Based Graphics Retrieval," *IET Electronic Letter*, vol. 46, no. 14, pp. 996-998, 2010.
- [43] Srivastava P. and Khare A., "Integration of Wavelet Transform Using Local Binary Patterns And Moments for Content-Based Image Retrieval," *Journal of Visual Communication and Image Representation*, vol. 42, pp. 78-103, 2017.
- [44] Tan X. and Triggs B., "Enhanced Local Texture Feature Sets for Face Recognition under Difficult Lighting Conditions," *IEEE Transactions Image Process*, vol. 19, no. 6, pp. 1635-1650, 2010.
- [45] Verma M. and Raman B., "Center Symmetric Local Binary Co-Occurrence Pattern for Texture, Face and Bio-Medical Image Retrieval," *Journal of Visual Communication and Image Representation*, vol. 32, pp. 224-236, 2015.
- [46] Wang X., Han T., and Yan S., "A HOG-LBP Human Detector with Partial Occlusion

Handling," in *Proceedings of IEEE 12th International Conference on Computer Vision*, Kyoto, pp. 32-39, 2009.

- [47] Yue J., Li Z., Lu L., and Fu Z., "Content-Based Image Retrieval Using Color and Texture Fused Features," *Mathematical and Computer Modelling*, vol. 54, no. 3-4, pp. 1121-1127, 2011.
- [48] Zhang B., Gao Y., Zhao S., and Liu J., "Local Derivative Pattern Versus Local Binary Pattern: Face Recognition With High-Order Local Pattern Descriptor," *IEEE Transactions on Image Processing*, vol. 19, no. 2, pp. 533-544, 2010.



Meenakshi Garg received her M.Tech. from MDU, Rohtak. She is expert in image processing and optimization fields. She has published research papers in various reputed journals. Currently, she is working as an Assistant Professor in Govt. Bikram College of Commerce, Patiala.



Manisha Malhotra received her Ph.D. from Maharishi Markandeshwar University, Mullana. She is expert in image processing, deep learning, and optimization fields. She has published more than 20 research papers in various indexed journals. Currently, she is working as an Professor in Chandigarh University, Gharoun, Chandigarh.



Harpal Singh received his Ph.D. from Punjabi University, Patiala. He is expert in image processing, deep learning, and optimization fields. He has published more than 10 research papers in various indexed journals. Currently, he is working as Professor in Chandigarh Engineering College, Landran, Chandigarh.